



ISSN: 0975-833X

## RESEARCH ARTICLE

### STRUCTURAL AND DIELECTRIC STUDIES OF COBALT FERRITE NANOPOWDER PREPARED BY CERAMIC METHOD

<sup>1</sup>Mehdi H. Diwan, <sup>1\*</sup>Nabeel A. Bakr and <sup>2</sup>Farid Jamali-Sheini

<sup>1</sup>Department of Physics, College of Science, University of Diyala, Diyala, Iraq

<sup>2</sup>Department of Physics, Ahwaz Branch, Islamic Azad University, Ahwaz, Iran

#### ARTICLE INFO

##### Article History:

Received 10<sup>th</sup> October, 2013

Received in revised form

26<sup>th</sup> November, 2013

Accepted 19<sup>th</sup> December, 2013

Published online 26<sup>th</sup> January, 2014

##### Key words:

Cobalt Ferrite, Ceramic Method,  
Spinel Phase, Dielectric constant,  
A.C. Conductivity.

#### ABSTRACT

Cobalt ferrite  $\{Co_x(Fe_2O_3)_{1-x}\}$  samples were prepared by conventional ceramic method with ferrite system ( $x = 0.29, 0.31, 0.33$  and  $0.35$ ). Structural measurements showed that all the samples of  $(CoFe_2O_4)$  have spinel phase structure. The other phase which has been observed belongs to  $(-Fe_2O_3)$ . The structural parameters such as interplanar distance ( $d$ ), lattice constant ( $a$ ) and grain size ( $D$ ) have been evaluated. X-Ray diffraction patterns showed that the crystal growth became stronger and more oriented and grain size became larger with increasing (Co) ratio. Dielectric measurements, A.C conductivity ( $\sigma_{ac}$ ), dielectric constant ( $\epsilon'$ ), and dielectric loss tangent ( $\tan \delta$ ) were measured in the frequency range ( $10^3$ Hz to 5MHz) at room temperature. All the samples show the normal dielectric dispersion. The dielectric constant ( $\epsilon'$ ) has a decreasing nature with frequency. This behavior is explained qualitatively in terms of the supposition that the mechanism of the polarization process in ferrite is similar to that of the conduction process.

Copyright © Mehdi H. Diwan et al. This is an open access article distributed under the Creative Commons Attribution License, which permits unrestricted use, distribution, and reproduction in any medium, provided the original work is properly cited.

## INTRODUCTION

Ferrites are very attractive materials for technological applications due to their combined properties as magnetic conductors (ferrimagnetic) and electric insulators. Polycrystalline ferrites, which have applications ranging from microwave frequencies to radio frequencies, are very good dielectric materials. The very low conductivity of these materials is very useful for microwave applications. Spinel ferrites, by virtue of their structure, can accommodate a variety of cations at different sites enabling a wide variation in electrical and magnetic properties. Cobalt ferrite ( $CoFe_2O_4$ ) possesses an inverse spinel structure and degree of inversion depends upon the heat treatment (Sawataky et al., 1968). Further  $CoFe_2O_4$  contains an isotropic magnetic ion  $Co^{2+}$ . The electrical and dielectric properties of materials substantially depend on the method of preparation (Gopalan et al., 2010), and heat treatment during preparation (Beitollahi et al., 2006), which controls the microstructure forming high resistive boundaries between the constituent grains. This leads to inhomogeneity in the structure and dielectric properties. Many workers have studied the structural, electrical and magnetic properties of cobalt ferrite and cobalt-substituted ferrite (Vilceanu et al., 2010; Hashim et al., 2009; Singh et al., 2010). It has been reported that the substitution of tetravalent ions in cobalt ferrite influences the structural, electrical and magnetic properties (Smit and Wijn 1959; Mohamed et al., 2010).

In the present study, we report our results on XRD-diffraction and dielectric properties of  $Co_x(Fe_2O_3)_{1-x}$  system with different percentages of Cobalt.

## MATERIALS AND METHODS

The samples of cobalt ferrite  $\{Co_x(Fe_2O_3)_{1-x}\}$  system were prepared through the usual doubled sintering ceramic method (Zhou et al., 2010) for ( $x = 0.29, 0.31, 0.33, 0.35$ ) using the analytical reagent grade of pure oxides, ( $-Fe_2O_3$ ) (Fluka, England, 99.99% purity),  $Co(NO_3)_2 \cdot 6H_2O$  (Fluka, England, 99.99% purity). The stoichiometric proportions of these oxides were thoroughly mixed manually together according to the chemical composition  $\{Co_x(Fe_2O_3)_{1-x}\}$  by using agate mortar for (1h) and fired in ( $800^\circ C$ ) for (2 hrs) by using a furnace (Alabtech -model LEF-1155-1- Korea). After that, the prepared samples inside the furnace were cooled for (24 hrs). The oxides of obtained compositions from pre sintering milled again by using (interrest electric mill) for (2 hrs) till a homogeneous mixture was obtained and riddled with a (75) micron diameter sieve to get ultrafine particles. The powder was pressed to form pellets of (10 mm) diameter by using (specac, England press) under pressure of ( $5 \text{ ton/cm}^2$ ) and finally sintered for (5 hrs) at ( $1100^\circ C$ ). The furnace subsequently is cooled to room temperature ( $20^\circ C/\text{min}$ ). Structural characteristics of samples were determined by X-ray diffraction patterns obtained in the ( $2\theta$ ) range of ( $20^\circ$ ) to ( $60^\circ$ ) using a Philips XRD-6000-Shimadzu diffractometer with ( $Cu K\alpha$ ) radiation ( $\lambda = 1.5406 \text{ \AA}$ ), operating at (40 kV) and (30mA). Dielectric measurements

\*Corresponding author: Nabeel A. Bakr

Department of Physics, College of Science, University of Diyala, Diyala, Iraq.

as a function of frequency in the range of (1 kHz – 5 MHz) were carried out using LCR meter (HP- 4284A) in conjunction with a laboratory designed cell in room temperature. The dielectric constant ( $\epsilon'$ ) is calculated using the following relation (Rani *et al.*, 2013):

$$\epsilon' = \frac{Cd}{\epsilon_0 A} \quad (1)$$

Where, C is capacitance, d is thickness of pellet,  $V_0$  is permittivity of the free space and A is cross sectional area of pellet. The dielectric loss ( $\epsilon''$ ) was calculated using the relation (Rani *et al.*, 2013):

$$v'' = \frac{1}{2f \cdot 1000 \cdot v_0} \quad (2)$$

Where  $\sigma$  is the a.c. conductivity.

The dielectric loss tangent ( $\tan\delta$ ) was calculated using the relation:

$$\tan \delta = \frac{\epsilon''}{\epsilon'} \quad (3)$$

## RESULTS AND DISCUSSIONS

### Structural Analysis

The XRD results of the cobalt ferrite nano powders  $\text{Co}_x(\text{Fe}_2\text{O}_3)_{1-x}$  system ( $x=0.29, 0.31, 0.33$  and  $0.35$ ) obtained from conventional ceramic method calcined at ( $1100^\circ\text{C}$ ) are depicted in Figure (1). The peaks at ( $30.12^\circ$ ,  $35.48^\circ$ ,  $37.11^\circ$ ,  $43.11^\circ$ ,  $53.51^\circ$  and  $57.01^\circ$ ) are indexed as the reflection planes of (220), (311), (222), (400), (422), and (511) respectively. The cobalt ferrite nano powders obtained reveal that all peaks are related to the ideal spinel cobalt ferrite phase (JCPDS: 22-1086) which confirms the presence of cobalt ferrite with a face-centered cubic structure (Jiang and Ai 2010). Our results show that the due to calcination at high temperature, the diffraction peaks become sharper and narrower, and their intensity increases. This indicates intensification in crystallinity that originates from the increment of crystalline volume ratio due to the particle size enlargement of the nuclei (Sui *et al.*, 2003). The impure phase of ( $\alpha\text{-Fe}_2\text{O}_3$ ) is found in all calcined samples.

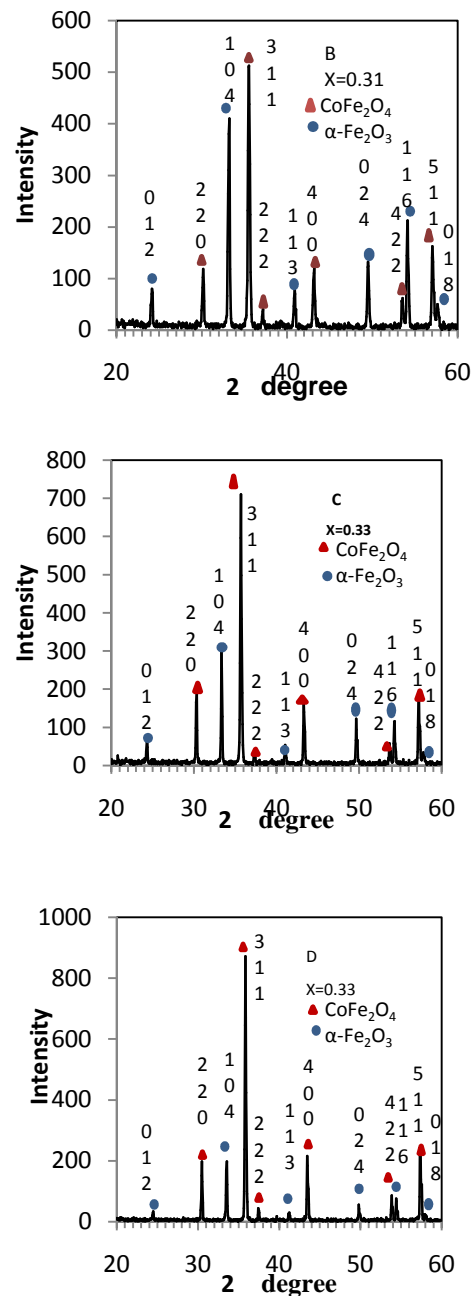
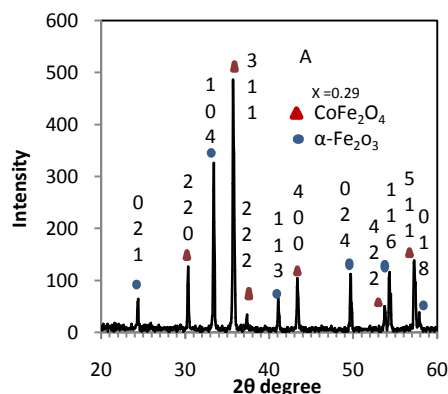


Figure 1. X-ray diffraction patterns for  $\text{Co}_x(\text{Fe}_2\text{O}_3)_{1-x}$  ( $x = 0.29, 0.31, 0.33$  and  $0.35$ ) nanoferrites samples at room temperature



This impurity occurs naturally as an impurity hematite phase (JCPDS: 33-0664) (Laokul *et al.*, 2011; Sanpo *et al.*, 2013). The values of the lattice parameter of the calcined samples obtained at ( $1100^\circ\text{C}$ ) are relatively in good agreement with the bulk value of  $8.377 \text{ \AA}$  (Jadhav *et al.*, 2008). The diffraction peaks are broad because of the nanometer size of the crystallite. The average particle size was determined from the full width at the half maximum (FWHM) of the XRD patterns, using the well-known Scherrer formula: (Kumar *et al.*, 2010).

$$D = K / \cos \quad (4)$$

Where (D) is the crystallite size (nm), ( $\Delta 2\theta$ ) is the full width of the diffraction line at half of the maximum intensity measured in radians, ( $\lambda$ ) is the X-ray wavelength of (Cu K  $\lambda = 0.154 \text{ nm}$ )

and  $\theta$  is the Bragg angle. The particle size estimated using the Scherer formula was found to increase with the increasing of cobalt ratio. The lattice parameter ( $a$ ) is calculated for prominent peak (311) using Bragg's equation.

$$a = \frac{d_{hkl}}{\sqrt{h^2 + k^2 + l^2}} \quad (5)$$

The calculated values of lattice parameter and crystallite size of all the samples are listed in Table (1).

Table 1. Crystallite size and Lattice parameter

Samples	Crystallite size D (nm)	Lattice parameter $\text{\AA}$ (nm)
$\text{Co}_{0.29}(\text{Fe}_2\text{O}_3)_{0.71}$	32.87	8.368
$\text{Co}_{0.31}(\text{Fe}_2\text{O}_3)_{0.69}$	48.65	8.325
$\text{Co}_{0.33}(\text{Fe}_2\text{O}_3)_{0.67}$	49.25	8.331
$\text{Co}_{0.35}(\text{Fe}_2\text{O}_3)_{0.65}$	54.69	8.295

The crystallite size was found to increase with increasing of cobalt ratio. It has been reported that the sintering process generally decreases lattice defects and strain, but this technique can cause the coalescence of smaller grains, resulting in an increased average grain size for the nano particles (Raming *et al.*, 2002). Calculated values of lattice parameter of cobalt ferrite samples were in good agreement with standard data (Smit and Wijn 1959).

## Dielectric measurements

### Dielectric Constant

The variation of dielectric constant as a function of frequency at room temperature from (1kHz to 5MHz) for cobalt ferrite samples  $\text{Co}_x(\text{Fe}_2\text{O}_3)_{1-x}$  where ( $x=0.29, 0.31, 0.33$  and  $0.35$ ) is shown in Figure (2). It is observed that the dielectric constant decreases with the increase in frequency and this is a normal dielectric behaviour of spinel ferrites, showing dispersion in low frequency range. All samples show dispersion due to Maxwell-Wagner (Maxwell 1973; Wagner *et al.*, 1913) and are also in agreement with the Koop's phenomenological theory (Koops 1951). The decrease in dielectric constant at higher frequency can be explained on the basis that the solid is assumed to be composed of well conducting grains and is separated by non conducting grain boundaries. When electrons reach such non conducting grain boundaries through hopping, and due to the high resistance of the grain boundary, the electrons pile up at the grain boundaries and produce polarization. At higher frequency beyond a particular limit, the electron does not follow the alternating field. This decreases the probability of electrons reaching the grain boundary and as a result the polarization decreases (Maxwell 1973; Koops 1951). The dielectric constant behavior is largely affected by (Cobalt) content. The decrease in dielectric constant with increasing (Co) content for samples with ( $x=0.33$  and  $0.35$ ) may be due to the migration of  $\text{Fe}^{3+}$  ions from octahedral site to tetrahedral site which decreases the hopping and hence decreases the polarization. However, the increase in dielectric constant for the samples with ( $x=0.29$  and  $0.31$ ) may be attributed to the formation of  $\text{Fe}^{2+}$  ions octahedral site, which increases the electron exchange between  $\text{Fe}^{2+}$  and  $\text{Fe}^{3+}$  and hence enhances the increase in the polarization, the increase in  $\text{Fe}^{2+}$  ions in octahedral site increases the hopping between  $\text{Fe}^{2+}$

and  $\text{Fe}^{3+}$  and hence increases the polarization. This results in the local displacement of electrons in the direction of applied field there by increasing the dielectric constant.

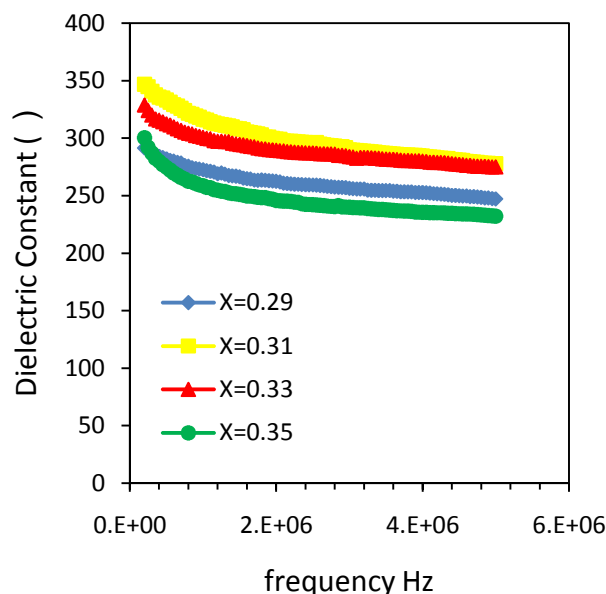


Figure 2. Variation of dielectric Constant ( $\epsilon'$ ) as a function of frequency at room temperature for  $\text{Co}_x(\text{Fe}_2\text{O}_3)_{1-x}$  nanoferrites

### Dielectric Loss

Figure (3) shows the variation of dielectric loss tangent  $\tan(\delta)$  as a function of the natural logarithm of frequency ( $\ln f$ ) at room temperature for cobalt ferrite  $\text{Co}_x(\text{Fe}_2\text{O}_3)_{1-x}$  system. In all samples, there is decrease in dielectric loss initially followed by resonance peak with increase in frequency where the dielectric loss in ferrite mainly originates from electron hopping and defect dipoles. The electron hopping contributes to the dielectric loss only in low frequency range. The response of electron hopping is decreased with increasing frequency and hence the dielectric loss decreases in high frequency range as shown in Figure (3). The charged defect dipoles contribute to the dielectric loss in high frequency range. Dielectric loss peaks can be observed for the samples with ( $x=0.29, 0.31, 0.33$  and  $0.35$ ) in the studied frequency range. The dielectric loss peak appears when the hopping frequency of the electron between  $\text{Fe}^{2+}$  and  $\text{Fe}^{3+}$  ions is close to the frequency of the external applied electric field. Furthermore, the loss peak in the figure moves to high frequency side with increase in Co content. This may be attributed to the fact that cobalt substitution prefers the octahedral site which strengthens the dipole-dipole interaction that restricts the rotation of the dipoles (Jadhav *et al.*, 2008). The decrease in dielectric loss tangent with increase in frequency is in accordance with the Koop's phenomenological model (Koops 1951). The dielectric loss arises if the polarization lags behind the applied alternating field and is caused by the presence of impurities and structural inhomogeneities. The value of dielectric loss tangent is very low in the present work indicating that the samples are structurally perfect (Rani *et al.*, 2013).

### A.C. Conductivity

Figure (4) shows the variation of a.c. conductivity ( $\sigma_{a.c.}$ ) as a function of the natural logarithm of frequency ( $\ln f$ ) at room

temperature. All samples show increase in conductivity as the frequency increases, which is the normal behaviour of ferrites. The conduction mechanism in ferrites can be explained on the basis of hopping of charge carriers between  $\text{Fe}^{2+}$  and  $\text{Fe}^{3+}$  ions on octahedral sites (Sathishkumar et al., 2010; Amarendra et al., 2002).

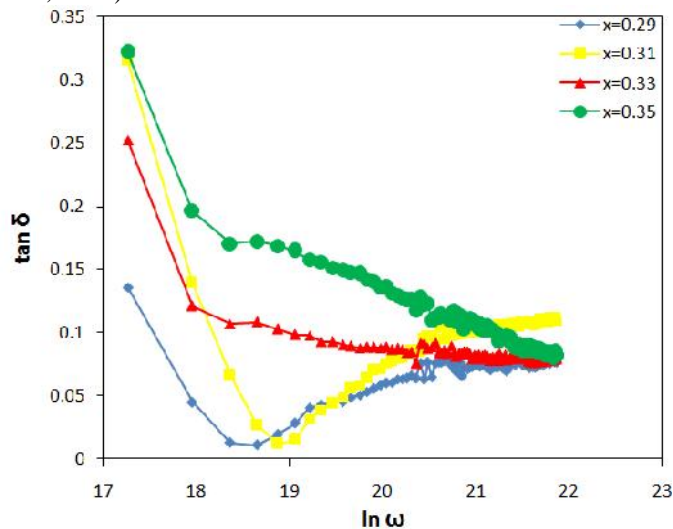


Figure 3. Variation of dielectric loss ( $\tan \delta$ ) as a function of the natural logarithm of frequency ( $\ln \omega$ ) at room temperature for  $\text{Co}_x(\text{Fe}_2\text{O}_3)_{1-x}$  nanoferrites

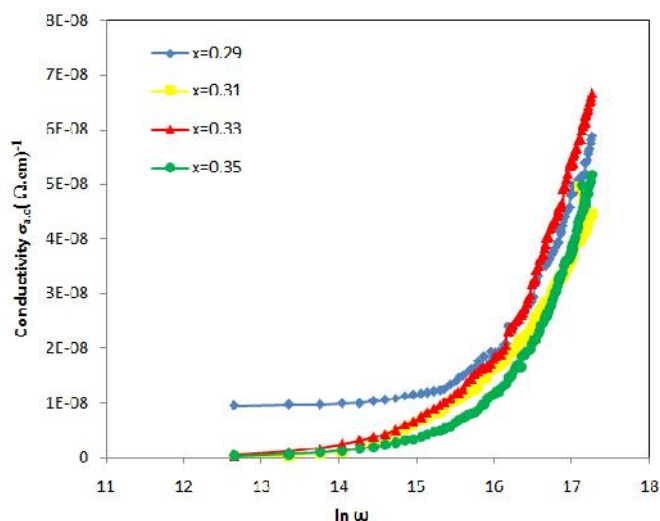


Figure 4. Variation of Conductivity  $\sigma_{a.c.}(\Omega.cm)^{-1}$  as a function of the natural logarithm of frequency ( $\ln \omega$ ) at room temperature for  $\text{Co}_x(\text{Fe}_2\text{O}_3)_{1-x}$  nanoferrites

## Conclusion

The study of structural properties of cobalt ferrite  $\{\text{Co}_x(\text{Fe}_2\text{O}_3)_{1-x}\}$  system prepared by the conventional ceramic method showed that the samples are spinel ferrite with a face-centered cubic structure. The decrease in dielectric constant with increasing (Co) content for samples with ( $x = 0.33$  and  $0.35$ ) may be due to the migration of  $\text{Fe}^{3+}$  ions from octahedral site to tetrahedral site which decreases the hopping and hence decreases the polarization. However, the increase in dielectric constant for the samples with ( $x = 0.29$  and  $0.31$ ) may be attributed to the formation of  $\text{Fe}^{2+}$  ions octahedral site. This behavior is explained qualitatively in terms of the supposition

that the mechanism of the polarization process in ferrite is similar to that of the conduction process (hopping).

## REFERENCES

- Amarendra K., T. Singh, C. Goel, R. G. Mendiratta, 2002. Dielectric Properties of Mn-Substituted Ni-Zn Ferrite, *Journal of Applied Physics*, Vol. 91, No. 10, p. 6626.
- Beitollahi A., R. Sani, Yu. V. Maksimov, I.P. Suzdalev, 2006. Structural and Magnetic Properties study of  $\text{CoFe}_2\text{O}_4$  Nanopowder prepared by Mechanical Milling using metallic Cobalt and Hematite powder Blend, *NSTI-Nanotech Vol. 1*, pp. 431-434.
- Gopalan V.E., I.A. Al-Omari, S.D. Kumar, Y. Yoshida, P.A. Joy, M.R. Anantharaman, 2010. Inverse magnetocaloric effect in sol-gel derived nanosized cobalt ferrite, *Appl. Phys. A: Materials Science & Processing*, 99(2), pp. 497–503.
- Hashim S.B.W.M., W.D.W. Yusoff, Z. Abbas, 2009. Physical and Magnetic Characterization of Polycrystalline Cobalt Ferrite ( $\text{CoFeO}$ ) Materials Prepared via Mechanically Alloyed Nanoparticles, *J. Applied Sciences Research*, 5(10), pp.1440-1444.
- Jadhav S., S. Shrisath, E. Sagar, B.G. Toksha, D.R. Shengule, K.M. Jadhav, 2008. Structural and Dielectric Properties of Ni-Zn Ferrite Nanoparticles Prepared by Co-precipitation Method, *J. Opto. Adv. Mater.*, 10. 2644-2648.
- Jiang J. and L. H. Ai, 2010. Synthesis and characterization of Fe-Co binary ferrosinell nanospheres via one-step nonaqueous solution pathway, *Materials Letters*, Vol. 64, No. 8, pp. 945–947.
- Koops C. G., 1951. On the dispersion of resistivity and dielectric constant of Some Semiconductors at Audio-frequencies, *Physical Review*, Vol. 83, p.121
- Kumar P., S.K. Sharma, M. Knobel, M. Singh, 2010. Effect of  $\text{La}^{3+}$  doping on electric, dielectric and magnetic properties of cobalt ferrite processed by co-precipitation technique. *J. Alloys compd*, 508, pp. 115–118.
- Laokul P., V. Amornkitbamrung, S. Seraphin, and S. Maensiri, 2011. Characterization and magnetic properties of nanocrystalline  $\text{CuFe}_2\text{O}_4$ ,  $\text{NiFe}_2\text{O}_4$ ,  $\text{ZnFe}_2\text{O}_4$  powders prepared by the Aloe vera extract solution, *Current Applied Physics*, Vol. 11, No. 1, pp. 101–108.
- Maxwell J. C., 1973. A Treatise on Electricity and Magnetism, Oxford University Press, New York, Vol. 1, p. 828.
- Mohamed R.M., M.M. Rashad, F.A. Haraz, W. Sigmund, 2010. Structure and magnetic properties of nanocrystalline cobalt ferrite powders synthesized using organic acid precursor method, *Journal of Magnetism and Magnetic Materials*, Vol. 322, Issue 14, pp 2058–2064.
- Raming T.P., A.J.A. Winnubust, C.M. Van Kats, P. Philipse, 2002. The synthesis and Magnetic Properties of nano sized Hematite particles. *J. Colloid Interface Sci.* 249, P. 346.
- Rani R., G. Kumar, K.M. Batoo, M. Singh, 2013. Electric and Dielectric Study of Zinc Substituted Cobalt Nanoferrites Prepared by Solution Combustion Method, *American Journal of Nanomaterials*, Vol. 1, No. 1, pp. 9-12.
- Sanpo N., J. Wang, C.C. Berndt, 2013. "Influence of Chelating Agents on the Microstructure and Antibacterial Property of Cobalt Ferrite Nanopowders", *Journal of the Australian Ceramic Society* Volume 49 (1), pp 84 – 91.

- Sathishkumar G., C. Venkataraju, K. Sivakumar, 2010. Synthesis, Structural and Dielectric Studies of Nickel Substituted Cobalt-Zinc Ferrite, *J. Materials Sciences and Applications* 1, pp.19-24
- Sawataky G.A., F.V.D. Woude, A.H. Morrish, 1968. Cation Distributions in Octahedral and Tetrahedral Sites of the Ferrimagnetic Spinel  $\text{CoFe}_2\text{O}_4$ , *J. Appl. Phys.* 39, 1204.
- Singh S., T. Namgy, S. Bansal, K. Chandra, 2010. Effect of Zn Substitution on the Magnetic Properties of Cobalt Ferrite Nano Particles Prepared Via Sol-Gel Route, *J. Electromagnetic Analysis & Applications*, 2, pp. 376-381.
- Smit J., H.P.J. Wijn, Ferrites, 1959. Philips Technical Library, Netherlands.
- Sui Y., X. Huang, Z. Ma, W. Li, F. Qiao, K. Chen, K. Chen, 2003. The effect of thermal annealing on crystallization  $\text{Si:H/SiO}_2$  multilayers by using layer by layer plasma oxidation, *Journal of Physics Condensed Matter*, Vol. 15, No. 34, pp. 5793–5800.
- Vilceanu V., M. Feder, L. Boutiuc, I. Dumitru, O.F. Caltun, 2010. The influence of chemical composition on initial permeability frequency spectra of cobalt ferrites, *Optoelectronics and Advanced Materials*, Vol. 4, No. 6, pp. 808 – 811.
- Wagner K. W., 1913. Zur Theorie der Unvollkommenen Dielektrika, *Annalen der Physik*, Vol. 40, pp. 817-855.
- Zhou J.P., L. Li, X.Z. Chen, 2010. Dielectric and magnetic properties of ZnO-doped cobalt ferrite, *Journal of Ceramic Processing Research*, Vol. 11, No. 2, pp. 263-272.

\*\*\*\*\*